Supporting Information

Dual-parameter sensing-visualization integration in a single electrochromic device for visual display

Xiaoran Liu[1], Jing Miao[1,2], Jiguang Chen[1], Mingshuo Zhen[3], Yingping Hong[1], Lei Liu[1,], Jijun Xiong, Chen Li[1,*]*

[1] State key Laboratory of Extreme Environment Optoelectronic Dynamic Measurement Technology and Instrument, State Key Laboratory of Widegap Semiconductor Optoelectronic Materials and Technologies and the Science and Technology on Electronic Test and Measurement Laboratory, North University of China, Taiyuan 030051, China

[2] the School of Mechanical Engineering, Suzhou University of Science and Technology, Suzhou 215009, China

[3] Department of Physics, School of Physics and Materials Science, Nanchang University, Nanchang 330031, China

∗ Corresponding Authors.

E-mail：liulei91@nuc.edu.cn (Lei Liu), lichen@nuc.edu.cn (Chen Li)

Content of Supporting Information

1. Raman shift of $ZnCl_2$ solutions with different concentrations

2. Fitted peaks of $ZnCl_2$ solutions with different concentrations

3. Solvation structure diagram of $ZnCl_2$ solution

4. Molality of $ZnCl_2$ aqueous solution as a function of the weight ratio of $ZnCl_2$ solutions to H_2O

5. Fabrication flowchart of $NbWO_x$

6. High resolution SEM of $NbWO_x$

7. CV and transmittance changes of $NbWO_x$ in different voltage ranges

8. Transmittance of $NbWO_x$ in 300-850 nm wavelength range under various $ZnCl_2$ concentrations

9. Transmittance of PANI in 300-850 nm wavelength range under various $ZnCl_2$ concentrations

10. Electrochromic Properties of PANI in $ZnCl_2$ solutions of different concentrations

11. High resolution SEM of $NbWO_x$ after 2000 cycles in $ZnCl_2$ solutions of different concentrations

12. Electrochemical performance of $NbWO_x$ in 5 M $ZnCl_2$ solution

13. Electrochemical performance of $NbWO_x$ in 10 M $ZnCl_2$ solution

14. Electrochemical performance of PANI in 5 M $ZnCl_2$ solution

15. Electrochemical performance of PANI in 7.5 M $ZnCl_2$ solution

16. Electrochemical performance of PANI in 10 M $ZnCl_2$ solution

17. Schematic about the *in-situ* measurement of devices

18. Transmittance modulation of the device with PANI electrode at different voltages

19. Output voltage at temperatures of 60 ℃ and 80 ℃

20. Output voltage at temperatures of 40% RH and 90% RH

21. Complete device color display

22. Transmittance change of dual-parameter sensing

23. More details on the color changes of the ZECDs

24. Reference

1. Raman shift of $ZnCl_2$ solutions with different concentrations

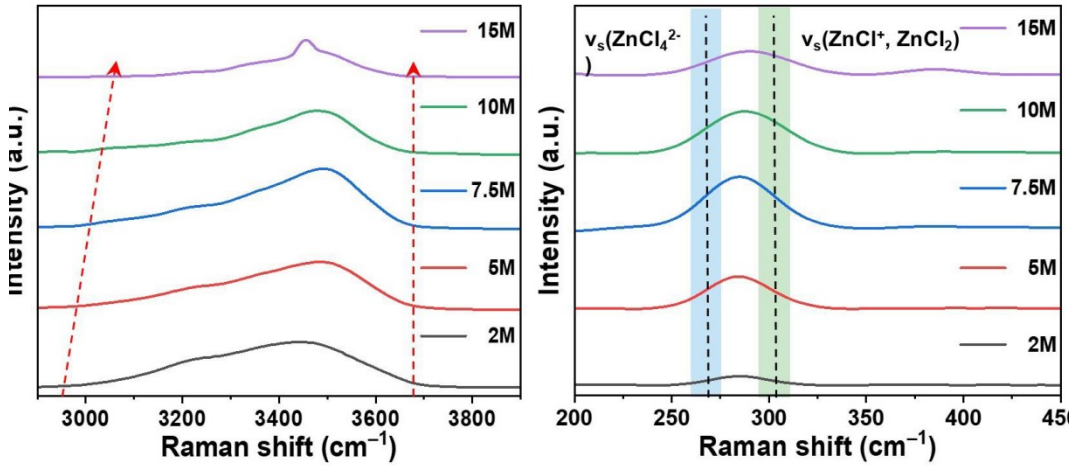

Figure S1. a) characteristics of O-H stretching vibration. b) solvation structure.

2. Fitted peaks of $ZnCl_2$ solutions with different concentrations

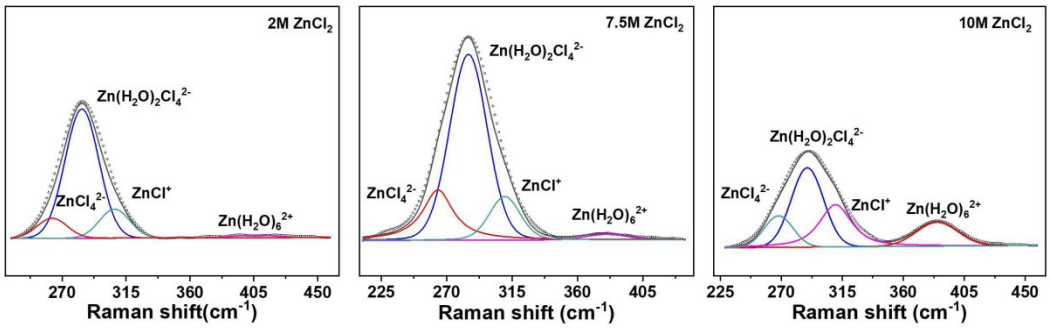

Figure S2. a)2 M $ZnCl_2$. b)7.5 M $ZnCl_2$. c)10 M $ZnCl_2$.

3. Solvation structure diagram of $ZnCl_2$ solution

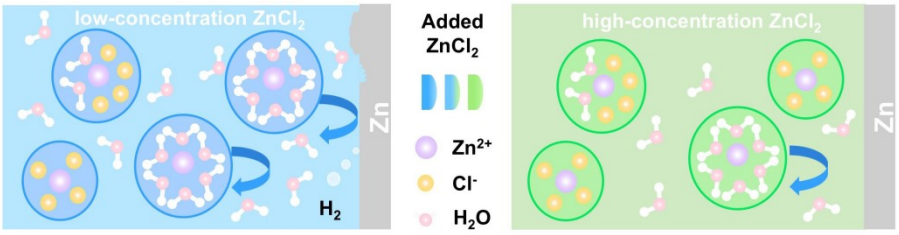

Figure S3. Solvation structure diagram of $ZnCl_2$ solution.

4. Molality of $ZnCl_2$ aqueous solution as a function of the weight ratio of $ZnCl_2$ solutions to H_2O

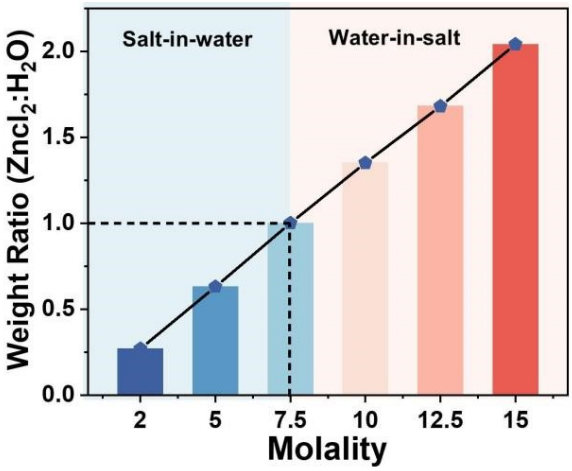

Figure S4. Molality of $ZnCl_2$ aqueous solution as a function of the weight ratio of $ZnCl_2$ to H_2O

5. Fabrication flowchart of $NbWO_x$

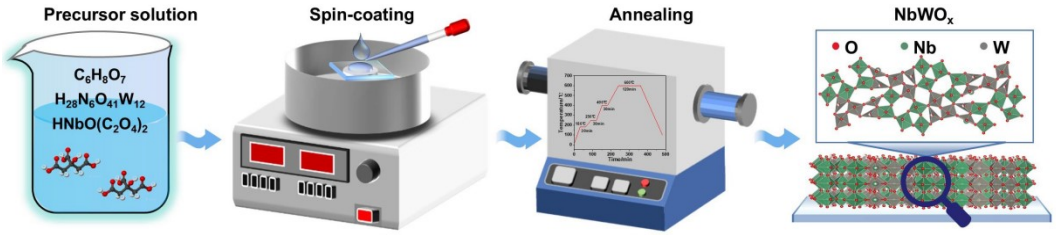

Figure S5. Fabrication flowchart of $NbWO_x$.

6. High resolution SEM of $NbWO_x$

High resolution SEM analysis revealed the highly ordered porous structure characteristics of the film, with uniform and interconnected pore size distribution.

Figure S6. High resolution SEM of $NbWO_x$.

7. CV and transmittance changes of $NbWO_x$ in different voltage ranges

Through CV and *in-situ* optical monitoring, the electrochemical behaviors and transmittance evolution of niobium-tungsten oxide electrodes under different potential windows were systematically investigated, and the optimal operating voltage window of the $NbWO_x$ electrode was determined to be -0.9 to 1.1 V.

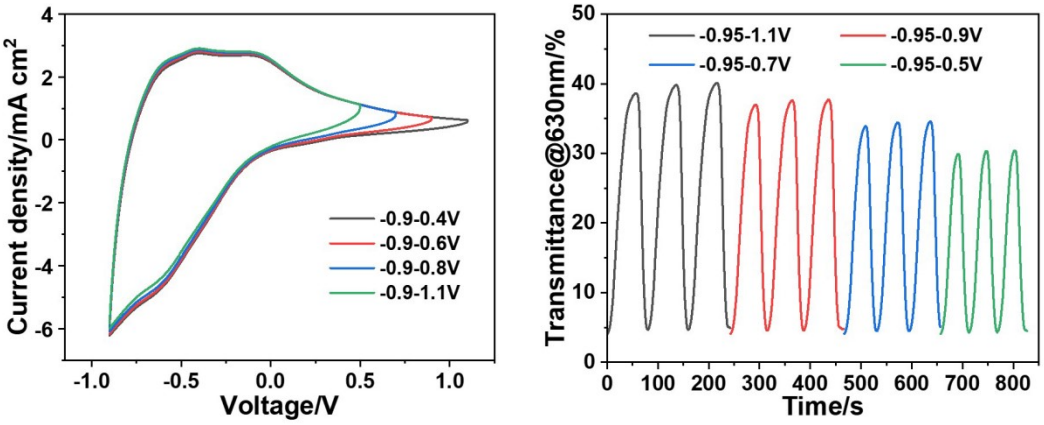

Figure S7. a) CV. b) transmittance.

8. Transmittance of $NbWO_x$ in 300-850 nm wavelength range under various $ZnCl_2$ concentrations

Figure S8 illustrates the evolution law of the electrochromic performance of $NbWO_x$ electrodes in $ZnCl_2$ electrolyte systems with different concentrations within the wavelength range of 300-850 nm. Through systematic characterization of the dynamic change characteristics of film transmittance under different applied voltage conditions, the structure-activity relationship between the optical modulation behavior of the electrode material and the electrolyte concentration is revealed.

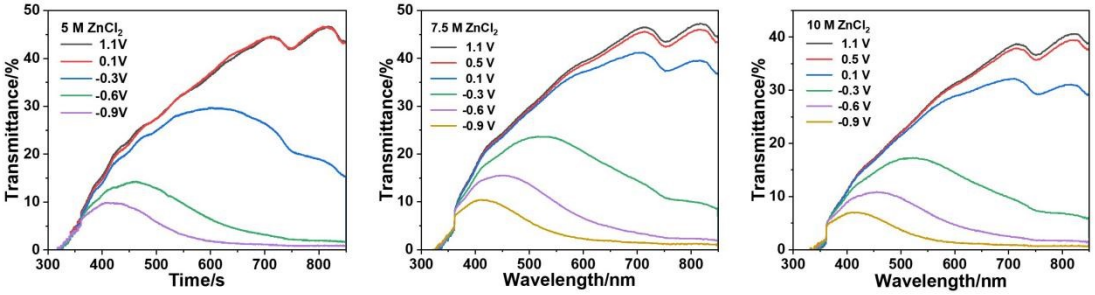

Figure S8. a) 5M $ZnCl_2$. b) 7.5M $ZnCl_2$. c) 10M $ZnCl_2$.

9. Transmittance of PANI in 300-850 nm wavelength range under various $ZnCl_2$ concentrations

Figure S9 demonstrates the electrochromic behavior of PANI electrodes in $ZnCl_2$ electrolyte solutions with varying concentrations across the 300-850 nm spectral range. The study systematically investigates the voltage-dependent transmittance modulation of the polymer films, elucidating the correlation between the optical switching properties and electrolyte composition.

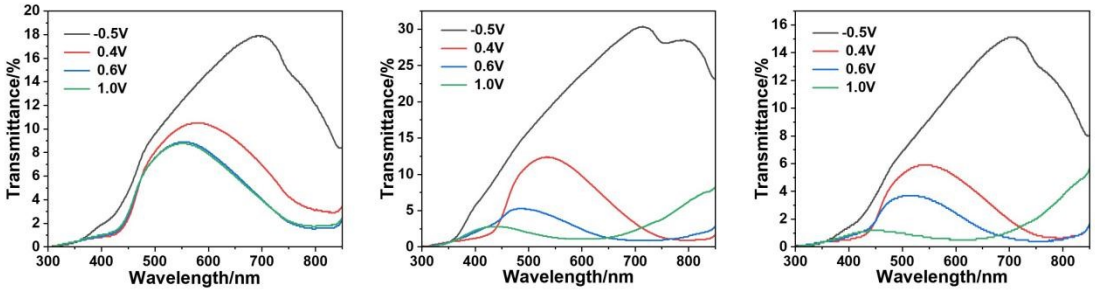

Figure S9. a) 5M $ZnCl_2$. b) 7.5M $ZnCl_2$. c) 10M $ZnCl_2$.

10 Electrochromic Properties of PANI in $ZnCl_2$ solutions of different concentrations

Through multi-concentration comparative experimental studies, the electrochromic performance of the PANI electrode in electrolyte systems with different $ZnCl_2$ concentrations was systematically characterized, specifically including transmittance spectral evolution, optical modulation amplitude, and cyclic stability within the wavelength range of 300-850 nm.

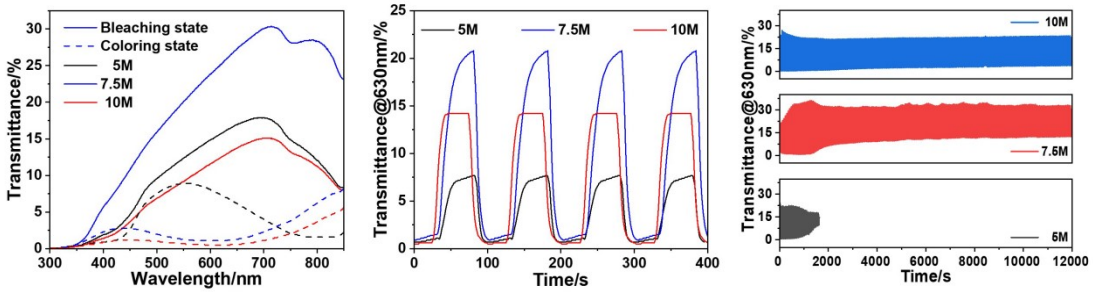

Figure S10. a) Bleached and colored state transmittance. b) *In-situ* transmittance response. c) Cyclic stability.

11. High resolution SEM of $NbWO_x$ after 2000 cycles in $ZnCl_2$ solutions of different concentrations

Furthermore, high resolution SEM was employed to characterize the morphological evolution of the thin films after 2000 electrochemical cycles, systematically investigating the influence of $ZnCl_2$ WIS electrolytes with varying concentrations (2 M, 7.5 M, and 10 M) on the structural stability of the films.

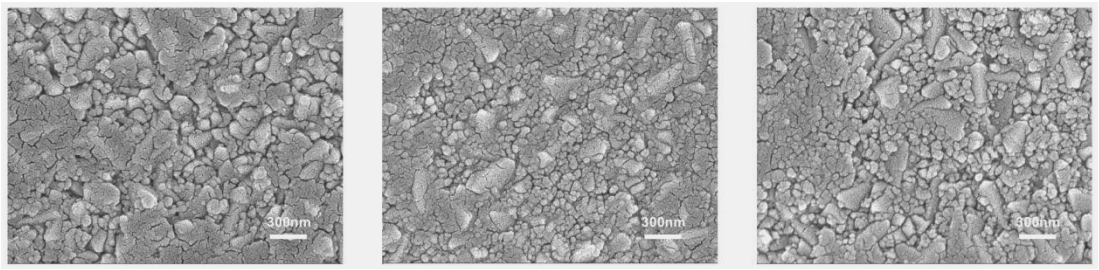

Figure S11. a) 5M $ZnCl_2$. b) 7.5M $ZnCl_2$. c) 10M $ZnCl_2$.

12. Electrochemical performance of $NbWO_x$ in 5 M $ZnCl_2$ solution

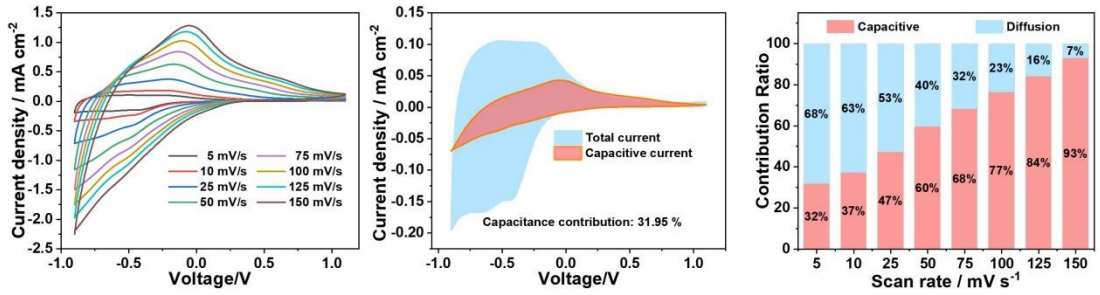

Figure S12. a) CV curves. b) surface at a scanning chamber rate of 5 mV/s contribution of capacitance to total current. c) percentage of diffusion control and surface capacitance behavior.

13. Electrochemical performance of $NbWO_x$ in 10 M $ZnCl_2$ solution

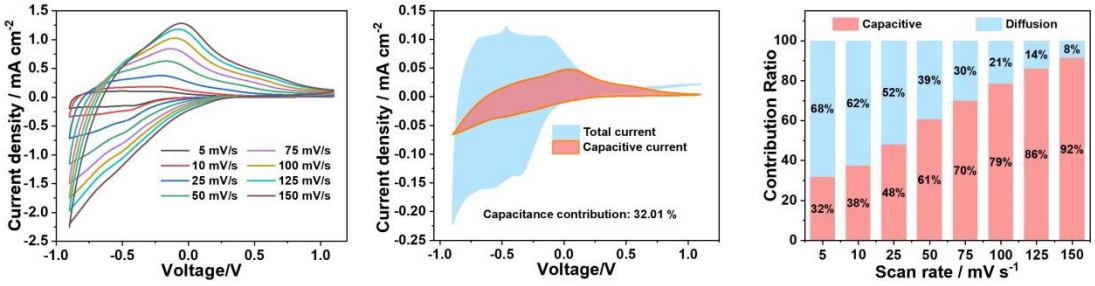

Figure S13. a) CV curves. b) surface at a scanning chamber rate of 5 mV/s contribution of capacitance to total current. c) percentage of diffusion control and surface capacitance behavior.

14. Electrochemical performance of PANI in 5 M $ZnCl_2$ solution

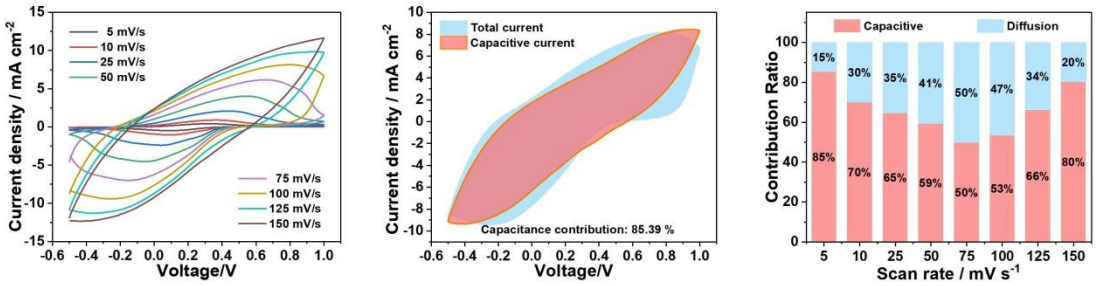

Figure S14. a) CV curves. b) surface at a scanning chamber rate of 5 mV/s contribution of capacitance to total current. c) percentage of diffusion control and surface capacitance behavior.

15. Electrochemical performance of PANI in 7.5 M $ZnCl_2$ solution

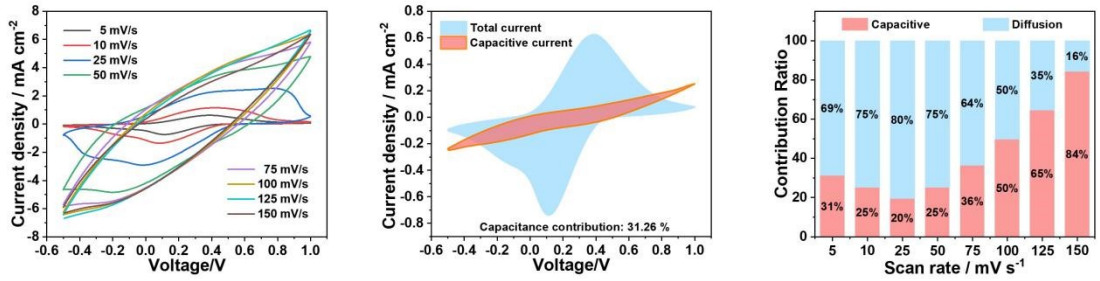

Figure S15. a) CV curves. b) surface at a scanning chamber rate of 5 mV/s contribution of capacitance to total current. c) percentage of diffusion control and surface capacitance behavior.

16. Electrochemical performance of PANI in 10 M $ZnCl_2$ solution

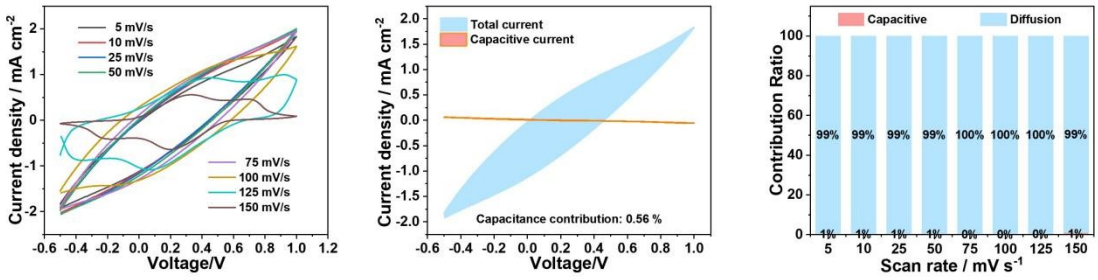

Figure S16. a) CV curves. b) surface at a scanning chamber rate of 5 mV/s contribution of capacitance to total current. c) percentage of diffusion control and surface capacitance behavior.

17. Schematic about the *in-situ* measurement of devices

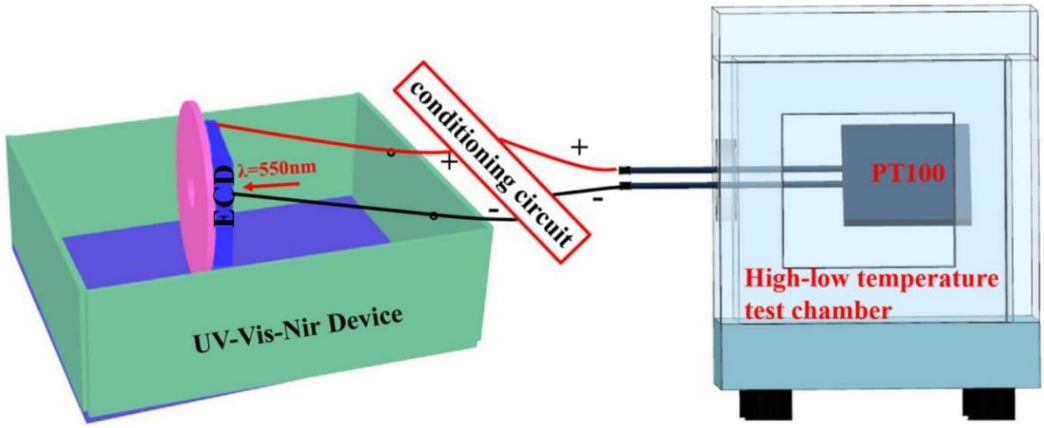

Figure S17. Schematic about the *in-situ* measurement of devices.

18. Transmittance modulation of the device with PANI electrode at different voltages

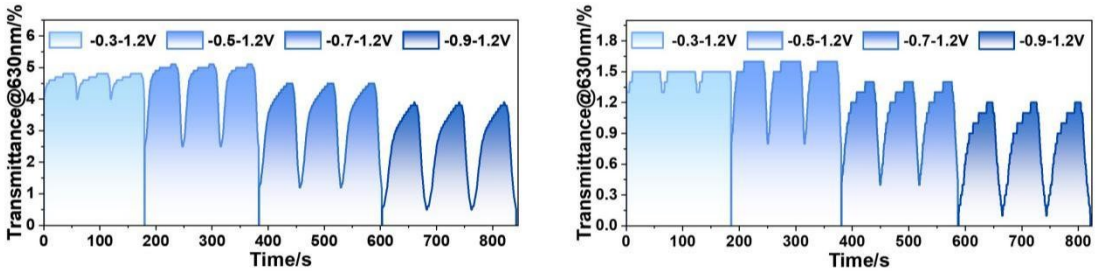

Figure S18. a) Temperature at 60℃. b) temperature at 80℃.

19. Output voltage at temperatures of 60 ℃ and 80 ℃

Figure S19. a) Temperature at 60°C. b) temperature at 80°C.

20. Output voltage at temperatures of 40% RH and 90% RH

Figure S20. a) Humidity at 40%RH. b) humidity at 90%RH.

21. Complete device color display

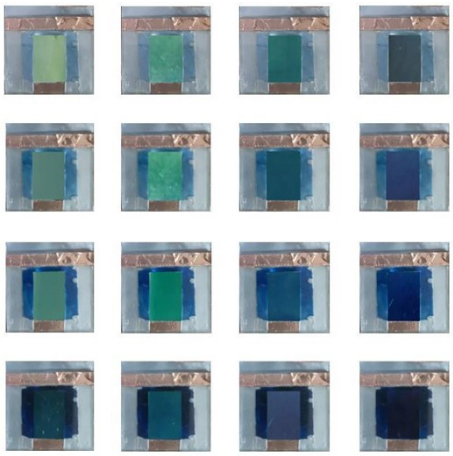

Figure S21. Complete device color display

22. Transmittance change of dual-parameter sensing

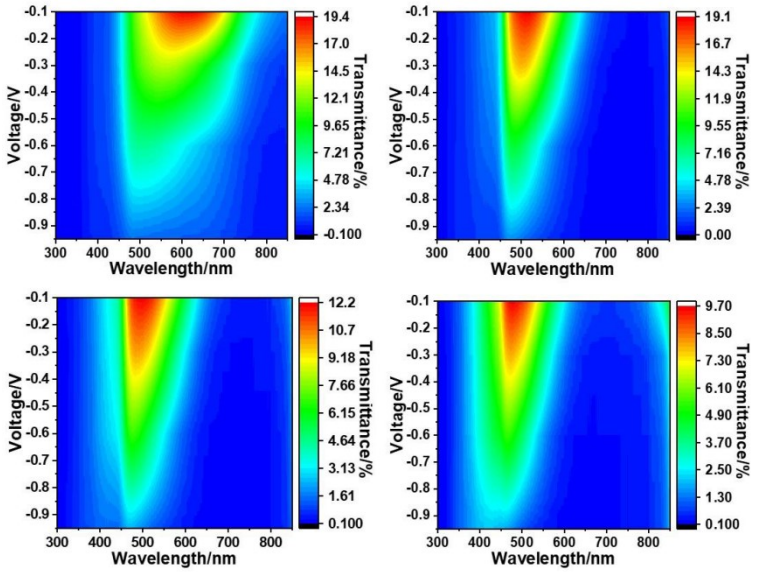

Figure S22. Transmittance change of dual-parameter sensing.

23. More details on the color changes of the ZECDs

Video S1 and **Video S2** recorded the dynamic color evolution process of the device under the conditions of "fixing the PANI electrode potential and regulating the $NbWO_x$ electrode potential" and "fixing the $NbWO_x$ electrode potential and regulating the PANI electrode potential", respectively, confirming the multicolor modulation capability of the as-prepared ZECD.

24. References

(1) Zhang, C.; Holoubek, J.; Wu, X.; Daniyar, A.; Zhu, L.; Chen, C.; Leonard, D. P.; Rodríguez-Pérez, I. A.; Jiang, J.-X.; Fang, C.; et al. A $ZnCl_2$ Water-in-salt Electrolyte for a Reversible Zn metal anode. *Chem. Commun.* **2018**, *54* (100), 14097-14099.

(2) Zhang Q.; Ma Y.; Lu Y.; Li, L. Modulating Electrolyte Structure for Ultralow Temperature Aqueous Zinc Batteries. *Nat. Commun.* **2022**, *11*, 4463.

(3) Mehmood, A.; Haidry, A. A.; Long, X.; He, W.; Zhang, X. Investigations on Niobium Tungsten Oxide Thin Films for Optical Modulation. *Journal of Materials Science* **2022**, *57* (9), 5361-5373.

(4) Wu, C.; Shao, Z.; Zhai, W.; Zhang, X.; Zhang, C.; Zhu, C.; Yu, Y.; Liu, W. Niobium Tungsten Oxides for Electrochromic Devices with Long-Term Stability. *ACS Nano* **2022**, *16* (2), 2621-2628.

(5) Ren, R.; Liu, S.; Gao, Y.; Lei, P.; Wang, J.; Tong, X.; Zhang, P.; Wang, Z.; Cai, G. Tunable Interaction Between Zn^{2+} and Superstructured $Nb_{18}W_{16}O_{93}$ Bimetallic Oxide for Multistep Tinted Electrochromic Device. *ACS Energy Lett.* **2023**, 2300-2307.

(6) Li, C.; Zhen, M.; Wang, K.; Liu, L.; Zhang, W.; Wang, Y.; Fan, X.; Hou, W.; Xiong, J. Temperature Sensors Integrated with an Electrochromic Readout toward Visual Detection. *ACS Appl. Mater. Interfaces* **2023**, *15* (34), 40772-40780.

(7) Zhang, W.; Li, H.; Elezzabi, A. Y. Electrochromic Displays Having Two-dimensional CIE color Space Tunability. *Adv. Funct. Mater.* **2021**, *32*, 2108341.